



**Intermittent attractive interactions lead to microphase separation in nonmotile active matter**Henry Alston <sup>1</sup>, Andrew O. Parry <sup>1</sup>, Raphaël Voituriez <sup>2,3</sup> and Thibault Bertrand <sup>1,\*</sup><sup>1</sup>*Department of Mathematics, Imperial College London, 180 Queen's Gate, London SW7 2BZ, United Kingdom*<sup>2</sup>*Laboratoire de Physique Théorique de la Matière Condensée,**UMR 7600 CNRS/UPMC, 4 Place Jussieu, 75255 Paris Cedex, France*<sup>3</sup>*Laboratoire Jean Perrin, UMR 8237 CNRS/UPMC, 4 Place Jussieu, 75255 Paris Cedex, France*

(Received 11 January 2022; accepted 26 July 2022; published 6 September 2022)

Nonmotile active matter exhibits a wide range of nonequilibrium collective phenomena yet examples are crucially lacking in the literature. We present a microscopic model inspired by the bacteria *Neisseria meningitidis* in which diffusive agents feel intermittent attractive forces. Through a formal coarse-graining procedure, we show that this truly scalar model of active matter exhibits the time-reversal-symmetry breaking terms defining the *Active Model B+* class. In particular, we confirm the presence of microphase separation by solving the kinetic equations numerically. We show that the switching rate controlling the interactions provides a regulation mechanism tuning the typical cluster size, e.g., in populations of bacteria interacting via type IV pili.

DOI: [10.1103/PhysRevE.106.034603](https://doi.org/10.1103/PhysRevE.106.034603)**I. INTRODUCTION**

All matter is built up from smaller components; active matter is no different. Often of biological inspiration, active matter generically denotes systems of particles which consume energy from their surroundings [1,2]. While this continuous consumption of energy leads to the breaking of time-reversal symmetry at the microscopic scale and thus maintains active systems out of equilibrium, striking nonequilibrium features generically stem from interactions between active particles or with their environment [3–5]. For instance, dense suspensions of interacting self-propelled particles display a wealth of phenomena forbidden by equilibrium thermodynamics including long-range order [6–10], clustering [11–14], or phase separation even in the absence of attractive interactions (e.g., motility-induced phase separation) [15–21]. Connecting emergent structures and collective dynamics to the behavior of individual particles through coarse-graining techniques remains an open problem which has seen recent development [22–27].

Equilibrium phase separation remains one of the simplest examples of order emerging from disorder, characterized by the spontaneous formation of regions with contrasting characteristics within a system. The dynamics of phase separation in a passive binary fluid are captured by Halperin and Hohenberg's *Model B* [28] which describes the evolution of a conserved scalar order parameter in a system respecting time-reversal symmetry (TRS) [29–32]. *Model B* itself can be derived from dynamical density functional theory (DDFT)—central to the analysis of passive, soft matter systems [33,34].

In contrast, recent works have focused on field theories capturing the TRS breaking present in active systems. Using a top-down approach, TRS violating terms can be added to

*Model B* equations to form a mean-field theory for motility-induced phase separation leading to the so-called *Active Model B* [35]. Interestingly, the addition in this active field theory of another term (of the same order in the expansion in the order parameter) leads to a second nonequilibrium field theory, *Active Model B+* (AMB+), which has been shown numerically and analytically to display microphase separation, driven by a *reverse* Ostwald ripening process [36–39]. The suppression of Ostwald ripening was also discussed in the context of coarse-grained models of *active emulsions* used to study phase separation in systems driven out of equilibrium, e.g., by chemical reactions [40–44].

In many-body physics, complex and robust collective behaviors can be the result of interactions between very simple constituent agents. While previous microscopic models have successfully produced the AMB+ phenomenology, these have focused on *motile* active matter—by far the most studied class of active systems. In contrast, minimal models of nonmotile—and in a sense *truly* scalar—active matter are crucially lacking in the literature, although they offer further examples of the nonequilibrium phenomena present in biological systems. Breaking from the motile active matter paradigm, we introduce in this article a minimal microscopic model of nonmotile particles whose interactions are governed by an *active* stochastic process and show that breaking TRS at the level of agent interactions can lead to striking consequences at the mesoscopic scale.

*Active switching* was previously introduced in microscopic models to generate particle shape changes [45], define the particle-particle interactions [46–48], a particle's interactions with an external field [49] or motility state [50,51]. Our model is inspired by the bacterium *Neisseria meningitidis* which interacts with its neighbors and environment through type IV pili, hairlike appendages whose contraction generates pulling forces [46,52]. In isolation, the bacterium extends and retracts its pili over time. Upon proliferation, the pili of neighboring bacteria touch; following contact, their retraction

\*t.bertrand@imperial.ac.uk

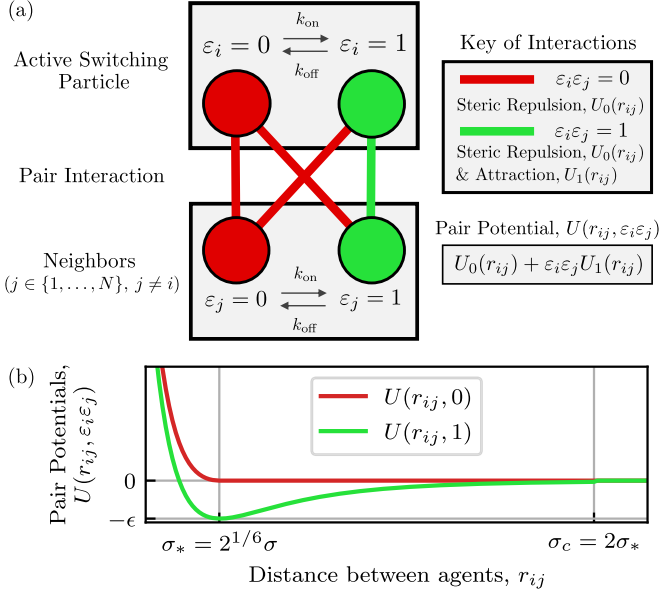


FIG. 1. Schematic of microscopic interactions. (a) The state of particle  $i$  is set by its internal variable,  $\varepsilon_i$ , which switches between 0 and 1 with fixed rates,  $k_{\text{on}}$  and  $k_{\text{off}}$ . The pair potential for neighboring particles depends on the product  $\varepsilon_i \varepsilon_j$ . (b) Pair potentials used in the simulations for  $\varepsilon_i \varepsilon_j = 0$  (red) and  $\varepsilon_i \varepsilon_j = 1$  (green). A WCA potential sets the particle size  $\sigma_*$  and the attraction range is set to  $\sigma_c = 2\sigma_*$  [56].

pulls pairs of bacteria together, eventually leading to bacterial clustering.

Recently, the mechanical properties of bacterial aggregates were explored using experiments and phenomenological continuum models [52–54]. In contrast, we describe minimally the pili interaction and introduce a model in which particles stochastically switch between attractive and purely repulsive states. We argue that this effective description loses none of the fundamental physics but allows for significant analytical progress. While the symmetries of our microscopic model are consistent with *Active Model B* and *B+*, a formal coarse-graining is required to conclude. We derive a density equation which we show is of *AMB+* form by identifying the TRS breaking terms [36,37]. Finally, we confirm the presence of microphase separation and reverse Ostwald ripening as predicted by the field theory by solving the kinetic equations numerically and compare these results to direct numerical simulations of the microscopic model, fully characterizing the nonequilibrium structure displayed by the system.

## II. MICROSCOPIC MODEL

### A. Theoretical model

We consider a system of  $N$  particles characterized by their position  $\mathbf{r}_i$  and an internal variable  $\varepsilon_i \in \{0, 1\}$  defining their interactions. Any two particles interact through steric repulsion when their center-to-center distance is such that  $|\mathbf{r}_i - \mathbf{r}_j| = r_{ij} < \sigma_*$ , independently of the value of  $\varepsilon_i$  and  $\varepsilon_j$ . If the internal variables of both agents are such that  $\varepsilon_i = \varepsilon_j = 1$ , these particles are additionally subjected to an attractive force with longer range  $\sigma_c > \sigma_*$  [see Fig. 1(a)]. We refer to

the case where  $\varepsilon_i = 1$  (respectively,  $\varepsilon_i = 0$ ) as the *on* state (respectively, the *off* state). We can define the total pair interaction potential as the superposition of purely repulsive  $U_0$  and purely attractive  $U_1$  contributions [see Fig. 1(b)]:

$$U(r_{ij}, \varepsilon_i \varepsilon_j) = U_0(r_{ij}) + \varepsilon_i \varepsilon_j U_1(r_{ij}). \quad (1)$$

The motion of the particles is governed by the overdamped Langevin equation

$$\dot{\mathbf{r}}_i = -\frac{1}{\gamma} \sum_{j \neq i} \nabla_{\mathbf{r}_i} U(r_{ij}, \varepsilon_i \varepsilon_j) + \sqrt{2D} \boldsymbol{\eta}_i, \quad (2)$$

where  $\gamma$  is a friction coefficient,  $D$  is the bare-diffusion coefficient which sets the temperature in the system, and  $\boldsymbol{\eta}_i$  is a zero mean, unit variance Gaussian white noise.

We introduce activity by allowing the particles to stochastically switch between the *on* and *off* states with constant rates, generically leading to intermittent attractive forces [Fig. 1(a)]. Formally, the internal variables  $\{\varepsilon_i\}_{i \in [1, N]}$  follow independent telegraph processes [55] with switching rates  $k_{\text{on}}$  and  $k_{\text{off}}$  (see [56] for details). Our model falls in the wide class of *nonmotile active matter* as the constituent agents are not self-propelled, but rather consume energy locally to change their interactions with neighboring agents.

### B. Simulations

First, we numerically solve the equation of motion [21,57]. The interaction potentials  $U_0$  and  $U_1$  are defined following the Weeks-Chandler-Anderson (WCA) decomposition [56,58]:

$$U_0(r_{ij}) = \begin{cases} 4\epsilon[(\sigma/r_{ij})^{12} - (\sigma/r_{ij})^6] + \epsilon, & r_{ij} < \sigma_* \\ 0, & r_{ij} \geq \sigma_*, \end{cases} \quad (3a)$$

$$U_1(r_{ij}) = \begin{cases} -\epsilon, & r_{ij} < \sigma_* \\ 4\epsilon[(\sigma/r_{ij})^{12} - (\sigma/r_{ij})^6], & \sigma_* \leq r_{ij} \leq \sigma_c \\ 0, & r_{ij} \geq \sigma_c. \end{cases} \quad (3b)$$

The results of our coarse-graining procedure below are insensitive to the specific choice of pair potential, provided that  $U_0$  is purely repulsive and divergent and  $U_1$  is attractive. Thus, we expect the results of our numerical simulations to be independent of the specific choice of potentials. To ensure that the system exhibits liquid-gas phase separation with no active switching, we work in the limit  $\epsilon \gg k_B T$ . Here, we restrict our focus to the case where  $k_{\text{on}} = k_{\text{off}} = k$  and keep the total volume fraction of agents fixed at  $\bar{\phi} = 0.3$ . We nondimensionalize the switching rate setting  $\kappa = k\sigma^2/D$ , where  $\sigma$  is the nominal particle diameter.

We quantify the structure in the numerical simulations using three metrics: the radius of gyration  $R_{\text{gyr}}$ , the demixing index  $I_{\text{demix}}$  and the size of the largest cluster  $s_{\text{max}}$ . The radius of gyration measures the average distance between a particle and the center of mass of the particles. We initialize each simulation with all the particles collected in a single drop, so if the radius of gyration remains generally constant in time, we conclude that the majority of particles are still near the center of the initial drop and the system is exhibiting full phase separation. If this measure increases significantly, then the initial configuration is not stable and the system is not sustaining full phase separation. The demixing index  $I_{\text{demix}}$  is defined as the fraction of neighboring particles in the same state, allowing

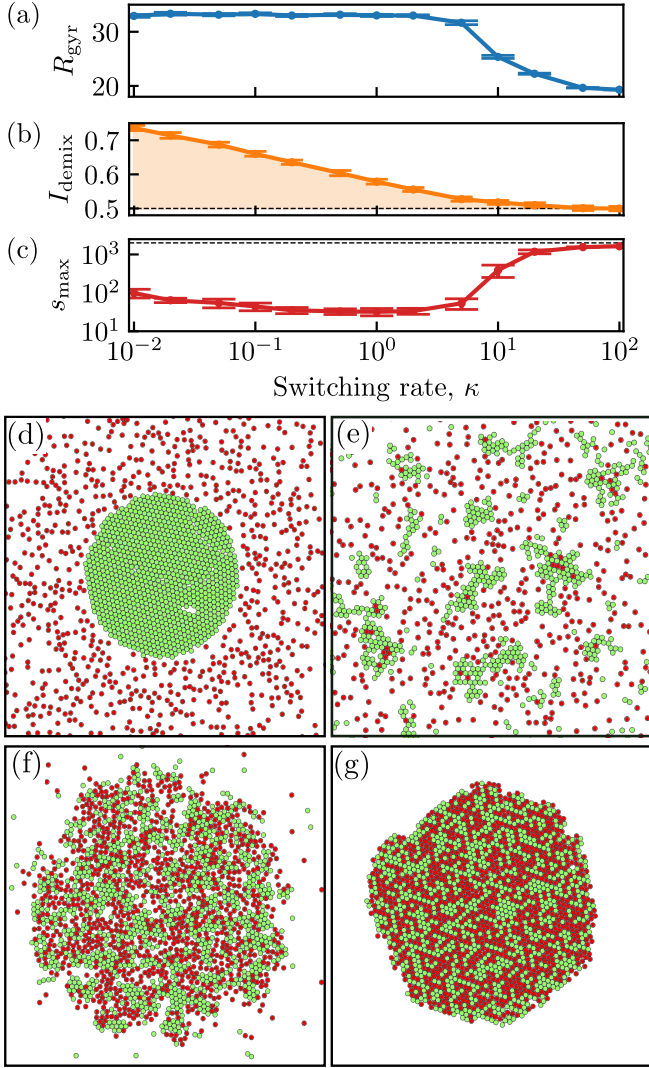


FIG. 2. Emergent structures in active switching system. (a) Radius of gyration  $R_{\text{gyr}}$ , (b) demixing index  $I_{\text{demix}}$ , and (c) maximal cluster size  $s_{\text{max}}$  for switching rates  $\kappa \in [10^{-2}, 10^2]$  and  $\epsilon \gg k_B T$ . Representative configurations obtained in simulations at steady state for (d)  $\kappa = 0$ , (e)  $\kappa = 10^{-2}$ , (f)  $\kappa = 10$ , and (g)  $\kappa = 100$ .

us to measure separation of *on* and *off* particles. Finally, we calculate the size of the largest cluster in the system  $s_{\text{max}}$ , which tells us whether the system is phase separating at all. Microphase separation is characterized by a large radius of gyration and a largest cluster size  $s_{\text{max}} \gg 1$ .

As we vary the switching rate between  $10^{-2} \leq \kappa \leq 10^2$ , we investigate the emergence of macroscopic structures (Fig. 2). At large switching rates  $\kappa \gg 1$ , the system fully phase separates and displays a single macroscopic drop as can be seen in Figs. 2(f) and 2(g); this is evidenced by a low radius of gyration  $R_{\text{gyr}}$  for  $\kappa \geq 10$  as well as a maximal cluster size  $s_{\text{max}}$  approaching the system size. Further, we observe that the stable drop is fully mixed with a demixing index  $I_{\text{demix}} \approx 0.5$ , defined as the fraction of neighboring particles in the same state [56]. For  $\kappa \gg 1$ , the diffusion timescale is much larger than the time between switching events; agents do not have time to diffuse out of reach

of the central drop before switching *on* and being pulled back.

As the switching rate decreases, both the radius of gyration and the demixing index monotonically increase. At low switching rates, the system does not reach full phase separation; instead, we argue that at intermediate switching rates our model exhibits *microphase* separation, where the system supports the coexistence of a large number of small clusters [Fig. 2(e)]. We conclude that the system demixes and self-organizes into clusters of *on* particles surrounded by a gas of *off* particles. The maximal cluster size reaches a minimum when  $\kappa \approx 1$  and increases again as we lower  $\kappa$ . Liquid-gas phase separation and demixing are strengthened as  $\kappa$  decreases. Indeed, longer times between switching events allow the nucleated clusters of attractive particles to grow further. In the singular limit where  $\kappa = 0$ , we observe a fully demixed state displaying a stable single drop of *on* particles surrounded by a diffusive gas of *off* particles. In the limit  $\epsilon \gg k_B T$ , the initial fraction of *on* particles controls the size of this drop as strong attraction ensures that *on* particles remain in the condensed phase.

### III. COARSE-GRAINING PROCEDURE

#### A. Many-body Smoluchowski equation

To quantify these structures analytically, we derive an equation for the particle density. Starting from a many-body Smoluchowski equation, an evolution equation for the  $N$ -agent distribution function  $\psi(\{\mathbf{r}_i, \varepsilon_i\}, t)$ , we explicitly coarse-grain our microscopic model by finding an approximate closure to the Bogoliubov-Born-Green-Kirkwood-Yvon hierarchy [see details in the Supplemental Material (SM) [56]]. We set  $\gamma = 1$  and write this equation as

$$\partial_t \psi_N = \sum_{n=1}^N \left[ \nabla_{\mathbf{r}_n} \cdot \left[ \sum_m \nabla_{\mathbf{r}_m} U(r_{nm}, \varepsilon_n \varepsilon_m) + D \nabla_{\mathbf{r}_n} \right] \psi_N + k S_n \psi_N - k \psi_N \right], \quad (4)$$

where  $r_{nm} = |\mathbf{r}_n - \mathbf{r}_m|$  and we have defined the operator  $S_i$  as

$$S_i \psi_N = \psi_N(\mathbf{r}_1, \dots, \mathbf{r}_N, \varepsilon_1, \dots, 1 - \varepsilon_i, \dots, \varepsilon_N). \quad (5)$$

Note that by definition  $S_i^2 \psi_N = \psi_N$ . We define the single-agent distribution function,  $\psi_1$ , as

$$\psi_1(\mathbf{r}, \varepsilon, t) = \sum_{\varepsilon_2=0}^1 \dots \sum_{\varepsilon_N=0}^1 \int d\mathbf{r}_2 \dots \int d\mathbf{r}_N N \psi_N, \quad (6)$$

where we have dropped the subscript on the tagged particle's position and internal variable.

We apply the same operations to the right-hand side of Eq. (4) as we did in Eq. (6), deriving an evolution equation for  $\psi_1$ :

$$\partial_t \psi_1(\mathbf{r}, \varepsilon, t) = \nabla_{\mathbf{r}} \cdot [D \nabla_{\mathbf{r}} \psi_1 - \mathbf{F}(\mathbf{r}, \varepsilon, t)] + k S_1 \psi_1 - k \psi_1, \quad (7)$$

where we have introduced the mean force on the tagged particle,  $\mathbf{F}$ , as

$$\mathbf{F}(\mathbf{r}, \varepsilon, t) = \sum_{\varepsilon'=0}^1 \int d\mathbf{r}' [-\nabla_{\mathbf{r}} U(r, \varepsilon\varepsilon')] \psi_2(\mathbf{r}, \mathbf{r}', \varepsilon, \varepsilon', t) \quad (8)$$

for  $r = |\mathbf{r} - \mathbf{r}'|$  and the two-agent distribution function,  $\psi_2$ .

We are left to approximate the mean force  $\mathbf{F}$ . Following a classical dynamical density functional theory (DDFT) approach valid in dense regimes where the structure of the fluid is dominated by hard-core interactions [30,34], we conclude that the mean force due to repulsive interactions on a particle in state  $\varepsilon \in \{0, 1\}$  is

$$\mathbf{F}_{\text{rep}}(\mathbf{r}, \varepsilon) = -\psi_1(\mathbf{r}, \varepsilon) \nabla \mu_{\text{rep}}[\rho(\mathbf{r})], \quad (9)$$

where we have defined the local density function as  $\rho(\mathbf{r}, t) = \sum_{\varepsilon=0}^1 \psi_1(\mathbf{r}, \varepsilon, t)$  and  $\mu_{\text{rep}}(\rho)$  is the chemical potential due to repulsive interactions, which can be written as the functional derivative of a free energy functional as in the DDFT equation [30,34] (see details in the SM [56]). For the contribution of the attractive interactions, we define  $\rho_\varepsilon(\mathbf{r}, t) = \psi_1(\mathbf{r}, \varepsilon, t)$  and make the mean-field approximation  $\psi_2(\mathbf{r}, \mathbf{r}', 1, 1, t) \approx \rho_1(\mathbf{r}, t) \rho_1(\mathbf{r}', t)$  for the two-agent distribution function, resulting in

$$\mathbf{F}(\mathbf{r}, 1) = \mathbf{F}_{\text{rep}}(\mathbf{r}, 1) - \rho_1(\mathbf{r}) \nabla (U_1 \star \rho_1), \quad (10)$$

where we have introduced the notation  $\star$  to represent a convolution between  $U_1$  and  $\rho_1$  [56]. This mean-field approximation is suitable as the attractive interactions are weak [30].

### B. Kinetic equations

At a macroscopic level, we find that the state of our system is described by the density fields  $\rho_0(\mathbf{r}, t)$  and  $\rho_1(\mathbf{r}, t)$  for the *off* and *on* particles, respectively. By (7), (9), and (10), the dynamics for these fields are governed by the kinetic equations

$$\partial_t \rho_0(\mathbf{r}, t) = \nabla \cdot \mathbf{J}_0 + s(\rho_0, \rho_1), \quad (11a)$$

$$\partial_t \rho_1(\mathbf{r}, t) = \nabla \cdot \mathbf{J}_1 - s(\rho_0, \rho_1), \quad (11b)$$

where the effect of the active switching is entirely contained in the coupling term  $s(\rho_0, \rho_1) = k(\rho_1 - \rho_0)$ . These kinetic equations are reminiscent of those seen in *reaction-diffusion density functional theory* (R-DDFT) models [33,45,47,49,59]. Self-diffusion and particle-particle interactions are expressed through the fluxes:

$$\mathbf{J}_0 = D \nabla \rho_0 + \rho_0 \nabla \mu_{\text{rep}}(\rho), \quad (12a)$$

$$\mathbf{J}_1 = D \nabla \rho_1 + \rho_1 \nabla \mu_{\text{rep}}(\rho) + \rho_1 \nabla (U_1 \star \rho_1). \quad (12b)$$

We note that although both *on* and *off* particles are subject to steric interactions, only *on* particles are subject to attractive interactions [last term in Eq. (12b)].

Interestingly, we note that in the case where  $k = 0$ , Eqs. (11) and (12) describe two classical equilibrium systems: a hard-sphere gas and a phase-separating Cahn-Hilliard-type fluid. Our results so far show that by coupling these two fluids, the resulting system can exhibit fundamentally nonequilibrium phase separation behaviors, including microphase separation. While this has been shown in previous studies

of *active emulsions* using phenomenological continuum models [40–43], we here derive a closed equation for  $\rho(\mathbf{r}, t)$  and show formally that it pertains to the AMB+ class.

## IV. AGENT DENSITY AND ACTIVE MODEL B+

### A. Closed equation for agent density

Starting from Eq. (11), we write an equation for the total density of particles

$$\partial_t \rho(\mathbf{r}, t) = \nabla \cdot \left[ \rho(\mathbf{r}) \nabla \left( \frac{\delta \mathcal{F}[\rho(\mathbf{r})]}{\delta \rho(\mathbf{r})} \right) + \rho_1(\mathbf{r}) \nabla (U_1 \star \rho_1) \right], \quad (13)$$

where although one cannot generically write a free-energy functional for active systems, we follow a common notation in field theories of active phase separation [35–37] and write the passive terms in our density equation as the gradient of the functional derivative of a free-energy-like functional

$$\mathcal{F}[\rho(\mathbf{r})] = \int d\mathbf{r} (D\rho(\mathbf{r}) \{\log[\rho(\mathbf{r})] - 1\} + f_{\text{rep}}[\rho(\mathbf{r})]), \quad (14)$$

where  $f_{\text{rep}}$  is the free-energy contribution due to repulsive interactions which satisfies  $f'_{\text{rep}}(\rho) = \mu_{\text{rep}}(\rho)$ .

The terms in this functional represent the local density approximations for the so-called *ideal gas* contribution and the contribution due to repulsive interactions. The attractive contribution, which contains implicitly the activity, contributes in (13) the necessary terms for our model to be of AMB+ form [36].

To show this, we first write Eq. (13) in closed form. The density of *on* particles is related to the density of all particles via  $\rho_1(\mathbf{r}) = \mathbb{P}(\varepsilon = 1 | \rho(\mathbf{r}) = \rho_b) \times \rho(\mathbf{r})$ , where this conditional probability can be seen as the fraction of particles in a region of bulk density,  $\rho \equiv \rho_b$  with internal variable  $\varepsilon = 1$ . We argue that this conditional probability is a function of the switching rate and the local total density, thus we define a function  $S_k(\rho) = \mathbb{P}(\varepsilon = 1 | \rho(\mathbf{r}) = \rho)$  to denote this functional dependence. We measure  $S_k(\rho)$  numerically in the simulations of our microscopic model for a wide range of switching rates as shown in Fig. 3. Here, we made a local density approximation and implicitly assume that the shape function  $S_k(\rho)$  does not depend on the gradient of the density field [30].

### B. Fast switching limit pertains to Model B

If switching happens much faster than diffusion,  $k \gg D/\sigma^2$ , then we argue that there should be no correlation between the particles local density and their state; we conclude that for large switching rates,  $S_k(\rho) \equiv \frac{1}{2}$ . In this case, we absorb the contribution of the attractive interactions to the probability current in a redefined free energy leading to a density equation of *Model B* form (see [56] for a full derivation). We conclude that the phase separation in this limit is driven by an effective attraction, with a quarter of its full strength, between any pair of agents leading to full phase separation as predicted by *Model B* [28].

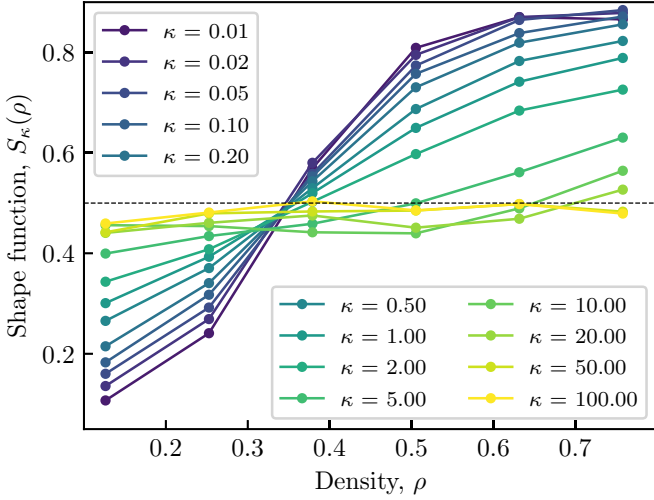


FIG. 3. Measuring  $S_k(\rho)$  numerically. Shape function  $S_k(\rho)$  measured from simulations of the microscopic model with nondimensional switching rates  $\kappa \in [10^{-2}, 10^2]$  and total volume fraction of agents  $\bar{\phi} = 0.3$  as the fraction of *on* agents in circular regions of radius  $\sigma_c$  with number of agents per unit area  $\rho$ .

### C. Fast (but finite) switching leads to Active Model B+

Here, we work perturbatively around the fast switching limit. When considering large but finite values of  $k$ , we perturb the shape function to linear order and write  $S_k(\rho) = 1/2 + A_k(\rho - \rho_c)$ , where we have defined  $\rho_c$  such that  $S_k(\rho_c) = 1/2$ . In doing so, we are implicitly modeling a small amount of demixing due to the finite switching rates. From our numerical analysis, we determine that  $\rho_c$  is independent of the switching rate  $k$  but may in general depend on other microscopic parameters.

After substituting this linear perturbation in the convolution in Eq. (13) and taking a gradient expansion of the nonlocal terms, we can rewrite the contribution of the attractive interactions to the current up to  $O(\nabla^4 \rho^3)$ . The coefficients of each of the TRS breaking terms are proportional to  $\mu_k = \frac{A_k}{4}(2\rho_c A_k - 1) \int d\mathbf{r} U_1(r)r^2$  [56]. Finally, we use the fact that adding a term of the form  $\alpha \rho |\nabla \rho|^2$  to the functional  $\mathcal{F}[\rho(\mathbf{r})]$  generates terms proportional to  $\alpha \nabla \cdot (|\nabla \rho|^2) - 2\alpha (\nabla \rho) \nabla^2 \rho - 2\alpha \rho \nabla^3 \rho$  in the current. Choosing  $\alpha = -3\mu_k/2$  and again redefining  $\mathcal{F}[\rho]$ , we write the density equation in the form

$$\partial_t \rho(\mathbf{r}, t) = \nabla \cdot \left\{ \rho(\mathbf{r}) \left[ \nabla \left( \frac{\delta \mathcal{F}[\rho(\mathbf{r})]}{\delta \rho(\mathbf{r})} - \frac{5\mu_k}{2} |\nabla \rho(\mathbf{r})|^2 \right) + \mu_k [\nabla^2 \rho(\mathbf{r})] \nabla \rho(\mathbf{r}) \right] \right\}. \quad (15)$$

Finally, we conclude that our model belongs to the AMB+ class, with constants  $\lambda = -5\mu_k/2 < 0$  and  $\zeta = -\mu_k < 0$  in the notation of Ref. [36].

### D. Active switching drives microphase separation

We expect to observe the emergence of microphase separation for a range of switching rates. We confirm this by numerically solving the R-DDFT equations (11) [56,60,61]. Specifically, we fix the total density of agents  $\bar{\rho}$  and size

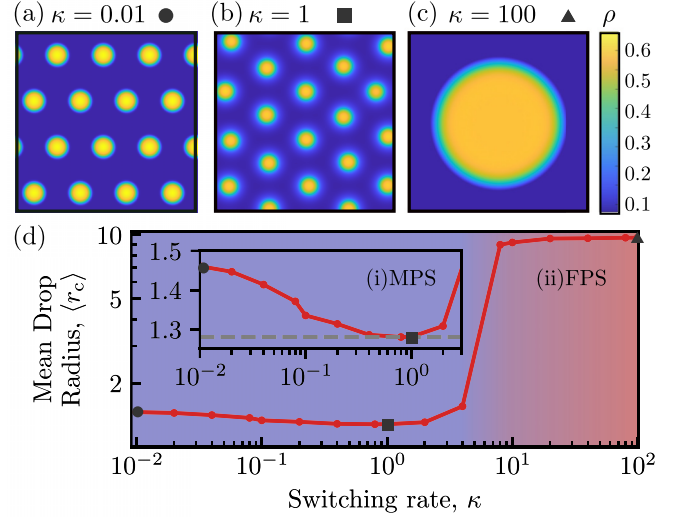


FIG. 4. Numerical analysis of kinetic equations. Numerical solutions of Eqs. (11) for  $\bar{\rho} = 0.16$  with  $\epsilon \gg k_B T$  [56]. Steady-state solutions show microphase separation (MPS) for (a)  $\kappa = 0.01$  and (b)  $\kappa = 1$  but full phase separation (FPS) for (c)  $\kappa = 100$ . (d) Mean droplet radius  $\langle r_c \rangle$  is nonmonotonic in the switching rate  $\kappa$  across the (i) microphase separated and (ii) full phase separated regimes, in agreement with Fig. 2(c).

of the solution domain and vary the switching rate  $\kappa$ . We set  $\epsilon \gg k_B T$  as to ensure phase separation from a nearly homogeneous initial condition. For moderate switching rates, the system's steady state supports the coexistence of droplets driven by a reversal of Ostwald ripening [56] (Fig. 4). Interestingly, droplet sizes are nonmonotonically controlled by the switching rate,  $\kappa$ . At higher switching rates, we observe full phase separation characterized by a single drop in the solution domain.

Note that the suppression of Ostwald ripening was first discussed in the context of active emulsions [40–42]. We confirm these phenomenological results through the proper coarse-graining of a minimal microscopic model. As argued above, at a macroscopic level, our system can be seen as a binary fluid driven away from equilibrium by active switching dynamics between the two components.

### V. MICROPHASE SEPARATION AND ACTIVE MODEL B+

Finally, we connect our two main results: our derivation of the AMB+ density equation used a perturbation of the fast-switching limit while the presence of microphase separation was shown for moderate switching rates. In particular, our linear approximation of the shape function is valid for any  $k$ , provided that  $|\rho - \rho_c|$  is small enough. This is sufficient to conclude on the classification of AMB+ for all switching rates  $k > 0$  [56].

To identify the conditions for microphase separation, we need to go beyond this linear perturbation. To do so, we make an ansatz for the functional form of  $S_k(\rho)$  motivated by our computational results (Fig. 3) that we argue is valid for all  $k$ . Using this ansatz, we evaluate the coefficients of the TRS breaking terms and compare them to [36] in which microphase separation in the (deterministic) AMB+ equation was first

studied. We find our results to be consistent for all switching rates [36,56].

Namely, for infinitely fast switching, one recovers an effective equilibrium field theory of Model B type with reduced attractive interactions. For fast (but finite) switching, shallow gradients in the shape function imply negative but small coefficients of the TRS breaking terms leading to full phase separation (FPS). For moderate switching rates, the gradient steepens generating large and negative coefficients leading to reverse Ostwald ripening and microphase separation (MPS). We argue that  $k$  controls how deep in the MPS region the system is and that the nonmonotonic dependence of the cluster size stems from the nonmonotonic behavior of  $\mu_k$  as we decrease  $k$  [56].

## VI. DISCUSSION

Using a bottom-up approach, we introduce a minimally active microscopic model inspired by type IV pili-mediated interactions. Through a rigorous coarse-graining procedure, we show that its density equation is of Active Model B+ form. We conclude that the switching rate associated with the pili-mediated interactions can set the typical cluster size in a system of bacteria such as *N. meningitidis*.

This nonmotile active matter system is shown to belong to the Active Model B+ class and exhibits microphase separation driven by a reversal of the Ostwald ripening process [36]. Further, we reveal in our model the existence of microphase separation, controlled by the switching rate  $k$ . In the con-

text of bacteria dynamics, intermittent attractive interactions mediated by pili dynamics lead to a mechanism controlling bacterial clustering and regulating typical cluster sizes. More generally, nonequilibrium field theories have been used to formally classify the emergence of self-organization and phase separation in active systems. Here, our coarse-graining allows us to connect microscopic models to these field theories and we believe that the current work lays the foundation for a more systematic study of microscopic active matter models.

In a field dominated by dry motile active matter models, we show here that the terms in the corresponding field theories breaking time-reversal symmetry, producing entropy, and thus leading to nonequilibrium collective behavior—such as microphase separation—can arise from models vastly different from the now classical self-propelled particles with steric repulsion as studied in the context of motility-induced phase separation. In contrast with those motile active matter models, the model we introduce here is *truly* scalar as activity does not translate to self-propulsion but rather is brought about by allowing the particles to dynamically change their interactions with their neighbors. In turn, our model breaks time-reversal symmetry in a manner which is preserving momentum conservation at the level of the interparticle interactions. While our study focuses on bacterial clustering, we believe our model has much wider applications and can, for instance, be used to model the dynamics of eukaryotic spheroids, in which our fluctuating forces would capture intercellular tension fluctuations [54,62].

- 
- [1] S. Ramaswamy, The mechanics and statistics of active matter, *Annu. Rev. Condens. Matter Phys.* **1**, 323 (2010).
  - [2] G. Gompper, R. G. Winkler, T. Speck, A. Solon, C. Nardini, F. Peruani, H. Löwen, R. Golestanian, U. B. Kaupp, L. Alvarez *et al.*, The 2020 motile active matter roadmap, *J. Phys.: Condens. Matter* **32**, 193001 (2020).
  - [3] M. C. Marchetti, J. F. Joanny, S. Ramaswamy, T. B. Liverpool, J. Prost, M. Rao, and R. A. Simha, Hydrodynamics of soft active matter, *Rev. Mod. Phys.* **85**, 1143 (2013).
  - [4] C. Bechinger, R. Di Leonardo, H. Löwen, C. Reichhardt, G. Volpe, and G. Volpe, Active particles in complex and crowded environments, *Rev. Mod. Phys.* **88**, 045006 (2016).
  - [5] T. Bertrand, Y. Zhao, O. Bénichou, J. Tailleur, and R. Voituriez, Optimized Diffusion of Run-and-Tumble Particles in Crowded Environments, *Phys. Rev. Lett.* **120**, 198103 (2018).
  - [6] T. Vicsek, A. Czirók, E. Ben-Jacob, I. Cohen, and O. Shochet, Novel Type of Phase Transition in a System of Self-Driven Particles, *Phys. Rev. Lett.* **75**, 1226 (1995).
  - [7] J. Deseigne, O. Dauchot, and H. Chaté, Collective Motion of Vibrated Polar Disks, *Phys. Rev. Lett.* **105**, 098001 (2010).
  - [8] A. Bricard, J.-B. Caussin, N. Desreumaux, O. Dauchot, and D. Bartolo, Emergence of macroscopic directed motion in populations of motile colloids, *Nature (London)* **503**, 95 (2013).
  - [9] A. P. Solon, H. Chaté, and J. Tailleur, From Phase to Microphase Separation in Flocking Models: The Essential Role of Nonequilibrium Fluctuations, *Phys. Rev. Lett.* **114**, 068101 (2015).
  - [10] T. Bertrand and C. F. Lee, Diversity of phase transitions and phase co-existences in active fluids, *Phys. Rev. Research* **4**, L022046 (2022).
  - [11] I. Theurkauff, C. Cottin-Bizonne, J. Palacci, C. Ybert, and L. Bocquet, Dynamic Clustering in Active Colloidal Suspensions with Chemical Signaling, *Phys. Rev. Lett.* **108**, 268303 (2012).
  - [12] I. Buttinoni, J. Bialké, F. Kümmel, H. Löwen, C. Bechinger, and T. Speck, Dynamical Clustering and Phase Separation in Suspensions of Self-Propelled Colloidal Particles, *Phys. Rev. Lett.* **110**, 238301 (2013).
  - [13] J. Palacci, S. Sacanna, A. P. Steinberg, D. J. Pine, and P. M. Chaikin, Living crystals of light-activated colloidal surfers, *Science* **339**, 936 (2013).
  - [14] T. Bertrand, J. d’Alessandro, A. Maitra, S. Jain, B. Mercier, R.-M. Mège, B. Ladoux, and R. Voituriez, Clustering and ordering in cell assemblies with generic asymmetric aligning interactions, [arXiv:2012.00785](https://arxiv.org/abs/2012.00785).
  - [15] J. Bialké, H. Löwen, and T. Speck, Microscopic theory for the phase separation of self-propelled repulsive disks, *Europhys. Lett.* **103**, 30008 (2013).
  - [16] T. Speck, J. Bialké, A. M. Menzel, and H. Löwen, Effective Cahn-Hilliard Equation for the Phase Separation of Active Brownian Particles, *Phys. Rev. Lett.* **112**, 218304 (2014).
  - [17] T. Speck, A. M. Menzel, J. Bialké, and H. Löwen, Dynamical mean-field theory and weakly non-linear analysis for the phase separation of active Brownian particles, *J. Chem. Phys.* **142**, 224109 (2015).

- [18] J. Zhang, R. Alert, J. Yan, N. S. Wingreen, and S. Granick, Active phase separation by turning towards regions of higher density, *Nat. Phys.* **17**, 961 (2021).
- [19] J. Tailleur and M. E. Cates, Statistical Mechanics of Interacting Run-and-Tumble Bacteria, *Phys. Rev. Lett.* **100**, 218103 (2008).
- [20] Y. Fily and M. C. Marchetti, Athermal Phase Separation of Self-Propelled Particles with No Alignment, *Phys. Rev. Lett.* **108**, 235702 (2012).
- [21] G. S. Redner, M. F. Hagan, and A. Baskaran, Structure and Dynamics of a Phase-Separating Active Colloidal Fluid, *Phys. Rev. Lett.* **110**, 055701 (2013).
- [22] H. Löwen, Inertial effects of self-propelled particles: From active Brownian to active Langevin motion, *J. Chem. Phys.* **152**, 040901 (2020).
- [23] M. E. Cates and J. Tailleur, Motility-induced phase separation, *Annu. Rev. Condens. Matter Phys.* **6**, 219 (2015).
- [24] F. D. C. Farrell, M. C. Marchetti, D. Marenduzzo, and J. Tailleur, Pattern Formation in Self-Propelled Particles with Density-Dependent Motility, *Phys. Rev. Lett.* **108**, 248101 (2012).
- [25] E. Bertin, M. Droz, and G. Grégoire, Hydrodynamic equations for self-propelled particles: Microscopic derivation and stability analysis, *J. Phys. A: Math. Theor.* **42**, 445001 (2009).
- [26] D. S. Dean, Langevin equation for the density of a system of interacting Langevin processes, *J. Phys. A: Math. Gen.* **29**, L613 (1996).
- [27] M. Schmidt, Power functional theory for many-body dynamics, *Rev. Mod. Phys.* **94**, 015007 (2022).
- [28] P. C. Hohenberg and B. I. Halperin, Theory of dynamic critical phenomena, *Rev. Mod. Phys.* **49**, 435 (1977).
- [29] A. J. Bray, Theory of phase-ordering kinetics, *Adv. Phys.* **51**, 481 (2002).
- [30] J.-L. Barrat and J.-P. Hansen, *Basic Concepts for Simple and Complex Liquids* (Cambridge University Press, Cambridge, UK, 2003).
- [31] H. Löwen, Melting, freezing and colloidal suspensions, *Phys. Rep.* **237**, 249 (1994).
- [32] P. M. Chaikin and T. C. Lubensky, *Principles of Condensed Matter Physics* (Cambridge University Press, Cambridge, UK, 1995).
- [33] M. te Vrugt, H. Löwen, and R. Wittkowski, Classical dynamical density functional theory: From fundamentals to applications, *Adv. Phys.* **69**, 121 (2020).
- [34] A. J. Archer and R. Evans, Dynamical density functional theory and its application to spinodal decomposition, *J. Chem. Phys.* **121**, 4246 (2004).
- [35] R. Wittkowski, A. Tiribocchi, J. Stenhammar, R. J. Allen, D. Marenduzzo, and M. E. Cates, Scalar  $\phi$ -4 field theory for active-particle phase separation, *Nat. Commun.* **5**, 4351 (2014).
- [36] E. Tjhung, C. Nardini, and M. E. Cates, Cluster Phases and Bubbly Phase Separation in Active Fluids: Reversal of the Ostwald Process, *Phys. Rev. X* **8**, 031080 (2018).
- [37] G. Fausti, E. Tjhung, M. E. Cates, and C. Nardini, Capillary Interfacial Tension in Active Phase Separation, *Phys. Rev. Lett.* **127**, 068001 (2021).
- [38] C. B. Caporusso, P. Digregorio, D. Levis, L. F. Cugliandolo, and G. Gonnella, Motility-Induced Microphase and Macrophase Separation in a Two-Dimensional Active Brownian Particle System, *Phys. Rev. Lett.* **125**, 178004 (2020).
- [39] X.-q. Shi, G. Fausti, H. Chaté, C. Nardini, and A. Solon, Self-Organized Critical Coexistence Phase in Repulsive Active Particles, *Phys. Rev. Lett.* **125**, 168001 (2020).
- [40] D. Zwicker, M. Decker, S. Jaensch, A. A. Hyman, and F. Jülicher, Centrosomes are autocatalytic droplets of pericentriolar material organized by centrioles, *Proc. Natl. Acad. Sci. USA* **111**, E2636 (2014).
- [41] D. Zwicker, A. A. Hyman, and F. Jülicher, Suppression of Ostwald ripening in active emulsions, *Phys. Rev. E* **92**, 012317 (2015).
- [42] J. D. Wurtz and C. F. Lee, Chemical-Reaction-Controlled Phase Separated Drops: Formation, Size Selection, and Coarsening, *Phys. Rev. Lett.* **120**, 078102 (2018).
- [43] C. A. Weber, D. Zwicker, F. Jülicher, and C. F. Lee, Physics of active emulsions, *Rep. Prog. Phys.* **82**, 064601 (2019).
- [44] S. C. Glotzer, E. A. Di Marzio, and M. Muthukumar, Reaction-Controlled Morphology of Phase-Separating Mixtures, *Phys. Rev. Lett.* **74**, 2034 (1995).
- [45] J. Grawitter and H. Stark, Feedback control of photoresponsive fluid interfaces, *Soft Matter* **14**, 1856 (2018).
- [46] D. Bonazzi, V. Lo Schiavo, S. Machata, I. Djafer-Cherif, P. Nivoit, V. Manriquez, H. Tanimoto, J. Husson, N. Henry, H. Chaté *et al.*, Intermittent pili-mediated forces fluidize *Neisseria meningitidis* aggregates promoting vascular colonization, *Cell* **174**, 143 (2018).
- [47] A. Moncho-Jordá and J. Dzubiella, Controlling the Microstructure and Phase Behavior of Confined Soft Colloids by Active Interaction Switching, *Phys. Rev. Lett.* **125**, 078001 (2020).
- [48] M. Bley, P. I. Hurtado, J. Dzubiella, and A. Moncho-Jordá, Active interaction switching controls the dynamic heterogeneity of soft colloidal dispersions, *Soft Matter* **18**, 397 (2022).
- [49] R. Zakine, J.-B. Fournier, and F. van Wijland, Field-Embedded Particles Driven by Active Flips, *Phys. Rev. Lett.* **121**, 028001 (2018).
- [50] M. Paoluzzi, M. Leoni, and M. C. Marchetti, Fractal aggregation of active particles, *Phys. Rev. E* **98**, 052603 (2018).
- [51] M. Paoluzzi, M. Leoni, and M. C. Marchetti, Information and motility exchange in collectives of active particles, *Soft Matter* **16**, 6317 (2020).
- [52] H.-S. Kuan, W. Pönisch, F. Jülicher, and V. Zaburdaev, Continuum Theory of Active Phase Separation in Cellular Aggregates, *Phys. Rev. Lett.* **126**, 018102 (2021).
- [53] K. Zhou, M. Hennes, B. Maier, G. Gompper, and B. Sabass, Non-equilibrium dynamics of bacterial colonies—Growth, active fluctuations, segregation, adhesion, and invasion, [arXiv:2106.06729](https://arxiv.org/abs/2106.06729).
- [54] D. Oriola, M. Marin-Riera, K. Anlas, N. Gritti, M. Sanaki-Matsumiya, G. Aalderink, M. Ebisuya, J. Sharpe, and V. Trivedi, Arrested coalescence of multicellular aggregates, *Soft Matter* **18**, 3771 (2022).
- [55] N. G. van Kampen, *Stochastic Processes in Physics and Chemistry*, 3rd ed. (North-Holland, Amsterdam, 2007).
- [56] See Supplemental Material at <http://link.aps.org/supplemental/10.1103/PhysRevE.106.034603> for more details on the coarse-graining procedure and numerical analysis.
- [57] A. C. Brańka and D. M. Heyes, Algorithms for Brownian dynamics computer simulations: Multivariable case, *Phys. Rev. E* **60**, 2381 (1999).

- [58] J. D. Weeks, D. Chandler, and H. C. Andersen, Role of repulsive forces in determining the equilibrium structure of simple liquids, *J. Chem. Phys.* **54**, 5237 (1971).
- [59] M. te Vrugt, J. Bickmann, and R. Wittkowski, Effects of social distancing and isolation on epidemic spreading modeled via dynamical density functional theory, *Nat. Commun.* **11**, 5576 (2020).
- [60] R. Roth, Fundamental measure theory for hard-sphere mixtures: A review, *J. Phys.: Condens. Matter* **22**, 063102 (2010).
- [61] S. Hermann, P. Krinninger, D. de las Heras, and M. Schmidt, Phase coexistence of active Brownian particles, *Phys. Rev. E* **100**, 052604 (2019).
- [62] S. Kim, M. Pochitaloff, G. A. Stooke-Vaughan, and O. Campàs, Embryonic tissues as active foams, *Nat. Phys.* **17**, 859 (2021).